Retraction

Retracted: Visualization of Low-Permeability Natural Core Carbon Dioxide Immiscible Flooding Flow Characteristics

Jie Chi; Jiabei Wang; Xing Zhang

IEEE Access

10.1109/ACCESS.2020.3007782

Notice of Retraction J. Chi, J. Wang, and X. Zhang, “Visualization of low-permeability natural core carbon dioxide immiscible flooding flow characteristics,” IEEE Access, vol. 8, pp. 142303–142311, 2020, doi: 10.1109/ACCESS.2020.3007782. After careful and considered review by a duly constituted expert committee, this article was retracted owing to irregularities in the peer review process, including acceptance for publication without the minimum number of independent reviews required by IEEE. The authors were contacted about the retraction and did not dispute it.

IEEE Access
Multidisciplinary | Rapid Review | Open Access Journal

Received May 22, 2020, accepted June 25, 2020, date of publication July 10, 2020, date of current version August 14, 2020.

Digital Object Identifier 10.1109/ACCESS.2020.3007782

Visualization of Low-Permeability Natural Core Carbon Dioxide Immiscible Flooding Flow Characteristics

JIE CHI[1], JIABEI WANG[2], AND XING ZHANG[3]

[1]School of Basic Sciences, Shengli College, China University of Petroleum, Dongying 257061, China
[2]School of Petroleum and Natural Gas Engineering, Chongqing Institute of Technology, Chongqing 401331, China
[3]Research Institute of Petroleum Engineering Technology, Shengli Oilfield Company, SINOPEC, Dongying 257000, China

Corresponding author: Jie Chi (chijie7980@126.com)

This work was supported in part by the Shandong Provincial Higher Education Research and Development Program (Science and Technology A Class) under Grant J18KA201, in part by the Chunhui Project of Shengli College of China University of Petroleum under Grant KY2017004, and in part by the High-Level Talent Research Start-Up Fund of Shengli College of China University of Petroleum under Grant KQ2019-008.

ABSTRACT Video image processing system is closely related to the development of modern science and technology. So visualization research is more and more important in the experiment. The main purpose of this paper is to study the feature visualization of CO_2 immiscible flooding seepage image of low permeability natural core. In this paper, particle image velocimetry PIV method and immiscible drive equation are used to realize the image acquisition of immiscible drive, and this paper is explored through the experiment of CO_2 immiscible drive percolation characteristics, analysis of immiscible zone migration characteristics, description and analysis of unsteady CO_2 immiscible drive experiment, and the production and analysis of percolation image visualization micro model. And in the result, the residual oil saturation of the heterogeneous model is 15.5% and 13.7%, which is not significantly higher than that of the homogeneous model, and the residual oil saturation is 35%. The conclusion is that the immiscible co permeability and the relative permeability curve of the reservoir with low viscosity and low permeability in the image visualization study. It makes a great contribution to the research of image visualization in the industrial development of low permeability natural core and improves the industrial production in the future.

INDEX TERMS Immiscible flooding, carbon dioxide seepage, image visualization, low permeability core.

I. INTRODUCTION

Due to the slow growth of China's oil and gas production in recent years, the degree of oil dependence on foreign countries is increasing rapidly year by year, among which the oil imports from the Middle East and other major countries account for 51%. In the case of emergency in the Middle East (war, etc.), blockade of the Persian Gulf and interruption of oil transportation, China can only provide 74.8 days (2.5 months) of oil, and energy use security is in danger. Compared with China, the supply of stationary oil in the United States can last 2146 days (more than 5 years and 10 months).

Improving the carbon dioxide technology of oil recovery is one of the effective methods to develop oil reservoirs, especially in low permeability oil reservoirs, high viscosity oil reservoirs and high shear oil reservoirs. Its effect is particularly important, and it is expected to become the third largest oil recovery alternative in the field of middle and later stage. This method has a wide application prospect. Considering the purpose of reducing carbon dioxide emissions, it can realize the development of environmental friendly green oil reservoir. The study of CO_2 enrichment includes the complex flow and displacement stability of porous fluid in porous media such as infiltration and dispersion. Therefore, it has important scientific and technical importance and application effect to start the experimental and simulation detection of CO_2 immiscible flood.

Injection of CO_2 into reservoir by Zhao x can improve oil recovery and promote CO_2 storage. He believes that for developing countries, the combination of EOR and CO_2 sequestration is an economic and environmentally safe way. His research introduces a CO_2 storage and EOR

The associate editor coordinating the review of this manuscript and approving it for publication was Zhihan Lv.

evaluation method to calculate the CO_2 storage potential of Daqing Oilfield. The energy storage coefficient, recovery coefficient and minimum miscible pressure (MMP) were determined by flow tube simulation and mixed element grid method. His experimental results show that CO_2 immiscible flooding can be carried out in most of Daqing oil fields. The average CO_2 storage factor of miscible flooding is 0.4, while the average CO_2 storage factor of miscible flooding is 0.28. Miscible flooding has better CO_2 storage capacity and enhanced oil recovery potential. The results show that CO_2 injection into Daqing Oilfield is a win-win technology [1]. The visualization of pseudo outcrops studied by mirkes e m demonstrates borehole and full diameter core images to enhance the ubiquitous cylinder view, thereby helping non professional translators. He believes that visualization is equivalent to the non-linear projection of images from the borehole to the earth's reference system, so as to generate the solid volume of longitudinal segmentation to reveal two or more surfaces, in which the direction of geological features indicates what is observed underground. An alternative to grain size is used to adjust the external size of the parcel to simulate the profile seen in the actual outcrop. The volume is created by a mixture of geological boundary elements and textures, which is the residual after subtracting the sum of boundary elements from the original data. In the case of using the wired microresistivity tool to measure, firstly, multi-scale direction conversion is used to repair the lost circumferential data. In this direction, the image is decomposed into its basic building structure, and then the complete image is reconstructed. Pseudo outcrop view can directly observe the angular relationship between features, and help to make visual comparison between borehole and core images, especially for non professionals interested in [2].

This paper mainly describes the principle and characteristics of immiscible flooding, PIV principle and technology of particle image velocimetry, basic principle of image processing and equation of immiscible flooding, and builds a visual experimental platform for CO_2 immiscible flooding, carries out the experiment of CO_2 immiscible flooding seepage characteristics, analyzes the experimental results, and combines the analysis of immiscible belt migration characteristics and unsteady CO_2 immiscible flooding The description and analysis of the miscible flooding experiment and the production and analysis of the microscopic model of the visualization of the seepage image jointly study the authenticity and effective demonstration of the intuitive data and situation brought by the visualization of the seepage image in this paper.

II. PROPOSED METHOD

A. PRINCIPLE AND CHARACTERISTICS OF IMMISCIBLE DRIVE

The general mechanism of immiscible flooding is limited by evaporation and displacement, the viscosity of crude oil decreases, crude oil expands, and the interfacial tension decreases.

Characteristics of immiscible phase drive [3], [4]:

(1) After mixing the solvents, some of them are dissolved in the reservoir fluid, and some of them remain as the upper phase, forming the relative body state.
(2) The formed upper phase moves forward and merges with many oil storage fluids to extract (extract) part of the intermediate hydrocarbon component from the oil storage fluid, or crude oil extracts part of the intermediate hydrocarbon component from the solvent. The components extracted from the upper phase are not enough to reach the mixed phase at the leading or trailing edge of the discharge.
(3) It is a single-phase system with high fluidity. The upper phase continues to flow forward, some of which is dissolved in the retention fluid, and then extracted from crude oil, or condensed intermediate hydrocarbon components from the upper layer, but it can never form.
(4) The recovery of crude oil is very low due to the fast fracture of the upper phase fluid. From the analysis of the gas injection mechanism of the crude oil improvement, it can be seen that the replacement process of different replacement methods is very different, and the factors affecting the replacement effect are also different.

B. CO_2 IMMISCIBLE DRIVE

CO_2 flooding technology as an effective EOR technology has been widely used in the world. It can achieve CO_2 emission reduction while flooding. For low-permeability reservoirs that conventional water injection may not be able to effectively develop, CO_2 flooding technology shows its incomparable advantages [5], [6].

In the study of immiscible flooding, firstly, according to the composition and properties of CO_2 / crude oil mixed system under immiscible flooding, a mathematical model of oil-gas percolation in a similar solution gas drive reservoir is established, then the percolation model is simplified and theoretically deduced, and the theoretical expression of the inflow dynamic equation of oil well is obtained. Then, the reservoir model is established to simulate the production of oil wells under the condition of immiscible flooding, and the inflow dynamic equation of oil wells with different CO_2 content is obtained. Then the dimensionless IPR equation under different CO_2 content is obtained by dimensionless treatment, finally, a non miscible oil well inflow performance curve and its corresponding equation are obtained by regression fitting of dimensionless IPR curve with different CO_2 content.

C. PARTICLE IMAGE VELOCIMETRY (PIV)

1) PIV TECHNOLOGY PRINCIPLE

PIV is a non-contact measurement method. The principle is to obtain the displacement value s of the set motion time interval T and the velocity u, that is, to calculate the cross-correlation between two pictures of the time interval T and obtain the displacement change of particles in the pictures. When the

carbon dioxide is put into the tracer particles, the density of the tracer particles should be similar to the density of the fluid to ensure that the motion of the tracer particles and the fluid is as consistent as possible, and the tracer particles should not be too small to ensure that the tracer particles have enough pixel expression on the camera. In the experiment, the tracer particles are prepared into a certain concentration of tracer particle suspension and put into the fluid. A double pulse laser generator is used to inject the laser from the side to illuminate the flow field. The tracer particles are illuminated twice in a very short period of time. When the laser is irradiated, the CCD is used to photograph synchronously. In this way, the particle images corresponding to the two laser beams are photographed and recorded on two different pictures. The camera is placed perpendicular to the laser to capture light scattered by particles. In this way, the velocity vector of the tracer particle can be calculated from the time interval of two laser beams and the displacement of the tracer particle [7], [8].

2) TRACER PARTICLE

In the PIV flow field measurement, in fact, the information between the frames of two photos is used to measure the displacement of particles. According to the information of the corresponding tidal current field, the selection of particles directly affects the quality of the measurement results. The tracer particles must have good compatibility and scattering close to the measurement of fluid density in the flow field [9], [10]. These properties are related to the property parameters of the particles themselves.

The scattering rate of tracer particles is one of the important factors affecting the quality of particle imaging. The larger the reflectivity is, the higher the contrast of imaging is, which is not only conducive to the clarity of imaging, but also conducive to the accuracy of flow field measurement. After years of research and development, the reflectivity of tracer particles is often increased by coating on the surface of tracer particles. The reflectivity of tracer particles after coating can reach more than 90%. In addition, particles with larger diameter can increase the scattering light intensity, thus improving the particle imaging quality [11], [12].

D. MMISCIBLE DISPLACEMENT EQUATION

1) PARTIAL FLOW EQUATION OF LOW PERMEABILITY CO_2 IMMISCIBLE FLOODING

The average pore throat radius of low permeability reservoir is relatively small, the contact between fluid and solid is strong, and the initial pressure changes in the process of permeability. Therefore, in the process of CO_2 enrichment in low permeability reservoirs, it is necessary to consider the consequences of the initial pressure change of oil phase. Now, one-dimensional permeability movement equation of oil phase and gas phase can be obtained [13], [14]:

$$\begin{cases} v_0 = -\dfrac{KK_{ro}}{\mu_0}\left(\dfrac{dp}{dx} + 0.1G_0\right) \\ v_g = -\dfrac{KK_{rg}}{\mu_g}\dfrac{dp}{dx} \\ v_0 + v_g = v_t = \dfrac{q}{A} \end{cases} \tag{1}$$

where: v_0, v_g refers to the seepage velocity of oil and gas phase, in cm/s; K refers to the permeability of formation, in D; G_0 refers to the opening pressure change of oil phase, in MPA/cm; v_t refers to the total seepage velocity of fluid, in cm/s; q refers to the injection capacity of CO_2, in cm^3/s; X refers to the horizontal axis coordinate, in cm; a refers to the partition area of seepage of reservoir, in cm^2. By substituting the oil and gas phase equations [15], [16], we can get:

$$\frac{dp}{dx} = -\frac{v_t/K + 0.1G_0\left(K_{ro}/\mu_0\right)}{\left(K_{ro}/\mu_0\right) + \left(K_{rg}/\mu_g\right)} \tag{2}$$

By combining the above two formulas, the partial flow equation of gas can be solved:

$$f_g = \frac{1}{1 + \left(K_{ro}/\mu_0\right)/\left(K_{rg}/\mu_g\right)}\left(1 + \frac{0.1KK_{ro}}{v_t\mu_0}G_0\right) \tag{3}$$

where: f_g is the partial flow of gas. According to the fitting of experimental data to discuss the answer, the formula of oil phase starting pressure change [17], [18]:

$$G_0 = a_0\left(\frac{1.0 \times 10^3 K}{\mu_0}\right)^{-n} \tag{4}$$

where: a_0, n refers to the experimental fitting coefficient, $a_0 = 1.2327$, n = 0.9754.

2) ROTATION PROGRESS OF CO_2 IMMISCIBLE DRIVE FRONT

In order to consider the dissolution of carbon dioxide to crude oil in the process of CO_2 enrichment, the B-L equation needs to be revised. The formula of CO_2 concentration in 1D CO_2 non piston displacement model is [19], [20] without considering the consequences of compressibility and gravity differential of crude oil and CO_2

$$\begin{cases} \dfrac{\partial C_{CO_2}}{\partial T_D} + \dfrac{\partial F_{CO_2}}{\partial x_D} = 0 \\ C_{CO_2} = S_g C_{CO_{2,g}} + S_0 C_{CO_{2,0}} \\ F_{CO_2} = f_g C_{CO_{2,g}} + \left(1 - f_g\right) C_{CO_{2,0}} \\ T_D = \dfrac{qB_g t}{\phi AL} \\ x_D = \dfrac{x}{L} \end{cases} \tag{5}$$

where: C_{CO_2} refers to the total concentration of carbon dioxide in the gas and oil phases; F_{CO_2} refers to the total carbon dioxide component capacity; TD refers to the injection time [21], [22]; XD refers to the dimensionless distance; $C_{CO_{2,g}}$, $C_{CO_{2,0}}$ refers to the concentration of carbon dioxide in the gas and oil phases; l refers to the length of the formation; ϕ refers to the porosity of the reservoir. The above equation is

a one-dimensional quasilinear equation, which can be substituted into the characteristic line method to get the answer. Displacement vector of carbon dioxide concentration profile:

$$v_D = \frac{dx_D}{dT_D} = \frac{dF_{CO_2}}{dC_{CO_2}} \tag{6}$$

Equation of equivalent change:

$$v_D = \frac{dF_{CO_2}}{dC_{CO_2}} = \frac{\Delta F_{CO_2}}{\Delta C_{CO_2}} = \frac{(F_{CO_2})_u - (F_{CO_2})_d}{(C_{CO_2})_u - (C_{CO_2})_d} \tag{7}$$

U is the upstream of the displacement front and D is the downstream of the displacement front. Equation of dimensionless displacement vector of front edge of carbon dioxide drive [23], [24]:

$$\begin{cases} v_D = \dfrac{\left[f_g C_{CO_{2,g}} + (1-f_g) C_{CO_{2,0}}\right] - 0}{(S_g C_{CO_{2,g}} + S_0 C_{CO_{2,0}}) - 0} \\ \quad \approx \dfrac{f_g - D_{0,g}}{S_g - D_{0,g}} = \left(\dfrac{df_g}{dS_g}\right) | S_{gf} \\ D_{0,g} = \dfrac{C_{CO_{2,0}}}{C_{CO_{2,0}} - C_{CO_{2,g}}} \end{cases} \tag{8}$$

$D_{0,g}$ is the diffusion retardation coefficient of carbon dioxide seepage. For the concentration of carbon dioxide in oil and gas phase, the equation [25]:

$$C_{CO_{2,0}} = \frac{R_{SO}}{22.4(R_{SO}B_g + 1)} \tag{9}$$

$$C_{CO_{2,g}} = \frac{1}{22.4B_g} \tag{10}$$

III. EXPERIMENTS

In this paper, MRI method is used to construct a visual experimental system of non mixed flow of carbon dioxide. The visual operating system and index determination methods are as follows. Visual operating system is divided into experimental materials and experimental device elements.

A. EXPERIMENTAL MATERIALS

In this experiment, glass sand particles are used to fill a cylindrical container to form a medium sample. The glass sand is made of quartz. This kind of glass sand is very lipophilic. Four kinds of glass sand (bz.01, bz.02, bz.04, bz.06) were selected in the scheme. Homogeneous sand filling model is composed of single sand with the names of bz.01, bz.02 and bz.04, while heterogeneous sand filling model is composed of mixed sand with the names of mz.2, mz.4 and MZ, respectively.

B. EXPERIMENTAL DEVICE

MRI system is mainly used to obtain the size of NMR signal and the sample fluid of imaging medium. The system is superconducting with high magnetic field and has the advantages of high image clarity and large signal to noise ratio. Its magnetic field intensity is 9.4T, frequency is 400MHz, and the highest magnetic field gradient is 50gauss / am. H micro imaging probe, computer with Linux operating system, data image processing system software.

The displacement system mainly uses light beam to complete the experiment of carbon dioxide immiscible filling tube. High pressure water pump, pressure conversion, thermal capacitance, phase filled with sand, vacuum air pump.

C. EXPERIMENTAL METHODS AND STEPS

In this paper, the basic operation of the automatic visualization scheme of CO_2 immiscible flooding under the condition of natural core is as follows:

(1) Fill the pipe with sand. Select full glass sand, measure sand fusion, slowly fill the glass sand model into the sand filled pipe, and knock the wall of the model filled pipe with a sand hammer at the same speed to achieve the corresponding role of fused sand. The sand addition pipe is compressed to be as close to the sand addition as possible.

(2) Temperature control of the injection pump. The inlet/outlet of the temperature control circulating device is connected to the temperature control tank of the injection pump by a hose, the device switch is opened, and the liquid in the pump is heated to the planned level.

(3) Pipe connection. Connect the oil pipeline according to the automation diagram of the scheme system, and do not connect the deviated pressure control device temporarily.

(4) Vacuum. In order to exhaust the vacuum pump in the whole device for 25 minutes, to reach the negative pressure of the pipeline, so that the sand is added to the sample in a vacuum.

(5) A model in which sand is added with saturated oil and test pressure. A certain flow rate of 0.2 ml per minute is used to inject sediment into the pipeline, so that the sample full of sand is completely saturated. Slowly pressurize to 20 MPa, provide a certain pressure, and confirm the leakage point. At the end of the pressure test, the 50mill part (70 $\sim$ 130nlltl) in the center of the 180 mm sand filling pipe is slowly placed, so that the central place where the sand is added to the sample becomes a strong electromagnetic field. The connecting back channel pressure control equipment is planned to be the pressure effect of the medium full of sand, so as to make the oil re saturated and rise to a certain pressure value stably.

(6) Temperature control of sand filling model. The equipment and facilities for temperature control interact with the circulating liquid port of the brake filled with sand to realize the circulating flow of the circulating liquid controlled by the temperature in the insulation instrument, turn on the switch circulating equipment, adjust the temperature of the experiment, and make the sample filled with sand reach a certain temperature.

(7) Image acquisition. When the temperature of the sand adding tube rises to the required temperature, the software system in the computer is acquired by image,

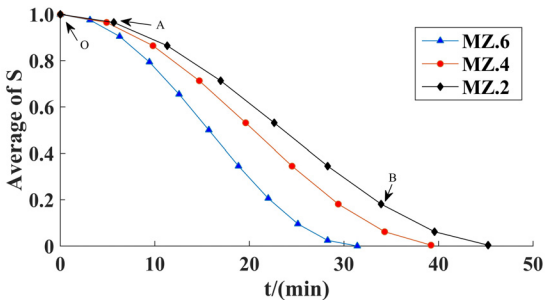

FIGURE 1. Change of global oil saturation of CO_2 immiscible flooding under different heterogeneities.

and the column and matching buttons under the probe are adjusted to complete the adjustment and dilution. Use the corresponding pulse data to adjust the data index. The selection of pulse data and the adjustment of index are as follows. Select RF excitation and layer as well as image of sample: perform phase and frequency procedures. That is, vertical actions are performed at the selected model level. Collect RF signal to get the initial data, synthesize photos, and convert the initial data into gray level photos.

(8) Miscible displacement. Add carbon dioxide into the sand with a certain flow rate, and conduct MR measurement together. After the displacement, stop the operation and obtain a series of photo data.

(9) Image processing. Discuss and calculate the photo data obtained from the review window of the system software.

(10) Disassemble the fuel line. Discharge and depressurize the carbon dioxide of the whole pipeline, decompose the channel path, clean the path for adding sand, and then act on the waste glass sand.

In this paper, the corresponding dynamic data of carbon dioxide mixing and enrichment process in media are observed, including oil saturation, size of immiscible region, displacement pre configuration and evolution progress of velocity in time and space.

IV. DISCUSSION

A. EXPERIMENTAL ANALYSIS OF IMAGE CHARACTERISTICS OF CO_2 IMMISCIBLE FLOODING SEEPAGE

Figure 1 shows 0.1ml/min, 8.5MPa and 37.8. Under the action of C, almost all the samples are not homogeneous. It still consists of three steps, the second of which is a straight segment. MZ. 6 has a shorter O-A phase than MZ. 2 and MZ. 4. In steps a to B, the ratio including the linearity of satisfaction is smaller than MZ. 2 and MZ. 4. The simulation data trend of the two sections of MZ. 2 and MZ. 6 is not homogeneous sample, as shown in Figure 1 below.

As shown in Fig. 1, this is the curve chart of the overall satisfaction change of CO_2 immiscible phase drive under various nonuniformities. In the B-C stage, the breaks of MZ. 2, MZ. 4 and MZ. 6 occurred at 38.4, 35.8 and 28.8 respectively. Compared with similar samples, the turning point of heterogeneous samples comes first. The satisfaction around the break point B slowly declines. This is due to the advance in the process of mixed replacement of heterogeneous samples and the turning point of replacement in advance. At present, when passing through the channel, because a little oil has not yet arrived, the drop of satisfaction will be stable. In this way, the recovery rate of different samples is much lower than that of similar samples. When the replacement is completed, the satisfaction of MZ. 2, MZ. 4 and MZ. 6 is composed of 13.4%, 15.2% and 14.3%. Compared with 13.7% of homogeneous samples, the residual satisfaction of heterogeneous samples did not increase significantly. In the sand samples, the non-uniformity caused by the fusion of sand particles with different particle sizes has little effect on the residual satisfaction. The reason is that the added sample belongs to non compaction medium, because there is no chromatography material, the dead docking base is small, and the docking connectivity is good. With the addition of samples from different structures, the total change area does not change much, and the remaining oil facies do not change much.

B. ANALYSIS OF MIGRATION CHARACTERISTICS OF IMMISCIBLE ZONE

Different experiments use different tracer particles. The selection of tracer particles is mainly based on the specific experimental situation. Because of different physical properties of gas and liquid, different tracer particles are used. See Table 1 for details.

Table 1 shows the information of missing particles commonly used in gas medium. The experiment was carried out in dark environment to minimize the impact of natural light on the shooting. The selected organic solvent is ethyl acetate, and the selected tracer particles need to be similar to the ethyl acetate solution. Therefore, magnesium oxide powder with good tracking performance and average particle size of 20 μ m is selected as the tracer particles in this experiment.

Changes in the length of the immiscible zone at different capacities of 0.2 ml / min, 0.25 ml / min, and 0.4 ml / min. Approximate the graph data and obtain the suspected table equation of the length of the non mixed region. In the 0.2 ml / min addition capacity, the distance of the non mixing zone is approximately the same, and the other equation is y = 7.31-0.02x. The throwing pressure rate of the length of the mixing zone is not very low, only 0.03 mm / min, which is almost zero. In the addition capacity of 0.16 ml / min, the addition equation of distance is y = 19.22-0.27x, and the reduction rate is 0.27 ml / min. The addition capacity of 0.3ml and the addition equation of distance are y = 24.32-0.62x. The descent speed is 0.62 mm per minute. This indicates that the range of distance variation in the non mixing region will increase with the increase of injection capacity. See Figure 2 for details.

As can be seen from Figure 2, after the injection capacity is increased, the satisfaction degree of the non mixed area

TABLE 1. Commonly used tracer particles in gaseous media.

Species	Material	The average diameter(μ m)
Solid	Polystyrene	0.5~10
	Alumina powder	0.2~5
	Magnesium oxide powder	0.1~5
	Solid glass ball	0.2~3
	Empty solid glass ball	30~100
	Synthetic paint particles	10~50
Liquid	Dioctyl phthalate	1~10
	Various oils	0.5~10
	Ethyl diacetate	0.5~1.5
	Helium filled soap bubbles	1000~3000

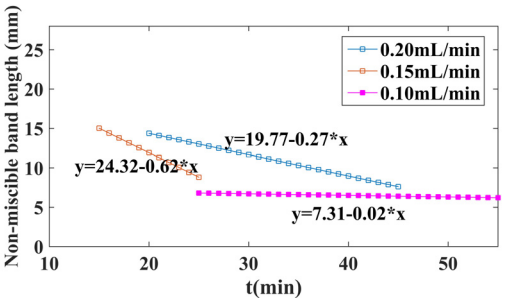

FIGURE 2. Change of the length of the non-miscible zone at different injection amounts.

TABLE 2. Core parameter table.

Feature	Parameter
Length/cm	4.39
Diameter/cm	2.52
Diameter/%	12.81
Gas permeability measurement/10^{-3} μ m^2	0.386
Bound water saturation/%	31.071

is more than 85%, first it becomes longer, then it becomes shorter, and then it becomes gentle at the end. The reason is that with the increase of the adding speed, the joint time between the bodies of the immiscible flow decreases, and the immiscible phase transition is unnecessary. With the development of displacement, immiscible phase drive is stable, and the distance of immiscible zone is shortened again. The phenomenon that the distance between the non mixed region first becomes longer and then shorter occurs mainly in the region where the degree of satisfaction of the non mixed region exceeds 85%.

C. DESCRIPTION AND ANALYSIS OF UNSTEADY CO_2 IMMISCIBLE FLOODING EXPERIMENT

According to the composition of the laminar flow body, sample fluid; wash and dry the rock samples, measure the geometric dimension and gas permeability; discharge the formation water, measure the porosity and rock samples, replace the heating equipment, and form the gradient method to make the temperature rise to 60 ° C, and maintain this temperature for 24 hours. A certain flow rate of 0.8cm^3 per minute is used to establish saturation oil and combined water saturation, so that the sealing pressure is always higher than the replacement pressure. After the water flow at the outlet is stable, determine the effective transmittance of the oil phase under the combined water saturation; record a certain flow rate of 0.8cm^3 per minute for CO_2 enrichment, displacement pressure at each time point, oil production and gas production; measure the effective gas transmittance under the remaining oil state until no gas overflows, until the end of the experiment. See Table 2 and figure 3 for details.

Table 2 is the parameter table of core.

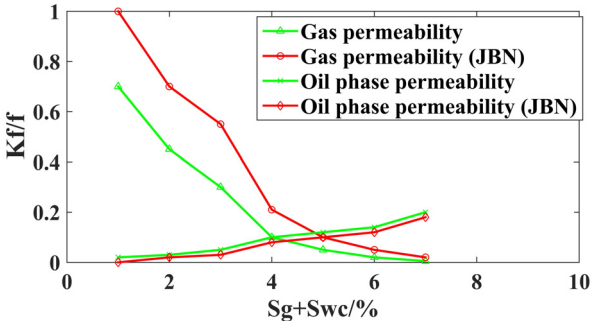

FIGURE 3. Typical percolation curve of immiscible carbon dioxide flooding in mountain storage layer.

As shown in Figure 3, the typical permeability curve of immiscible carbon dioxide drive in the mountain reservoir shows the following characteristics: under low gas saturation, the relative permeability of oil phase decreases rapidly with the increase of gas saturation, while the relative permeability increases slowly, and the permeability of gas phase increases rapidly. The end value of gas phase permeability is a little low, less than 0.1. This shows that the gas permeability is relatively weak. The saturation characteristic values of combined water and residual oil are 35% and 30% respectively, indicating that the immiscible and immiscible displacement of carbon dioxide is limited. The range of two-phase region is about 35%, which shows that the co permeability and space of two-phase are limited. In addition, the characteristics of relative permeability curves of low viscosity and low permeability reservoirs.

Compared with the conventional ''JBN'' method for calculating relative permeability, the calculation results of this model are obviously different. The relative permeability of the oil phase increases greatly. The permeability of gas phase is greatly reduced. The saturation degree of combined gas is relatively decreased. The differences reflected by this model play an important role in the analysis of reservoir engineering. Therefore, the permeability model, carbon dioxide dissolution and viscosity reduction of crude oil and gas phase slippage effect are the aspects that can not be forgotten in calculating the relative transmittance.

D. PRODUCTION AND ANALYSIS OF THE MICRO MODEL OF SEEPAGE IMAGE VISUALIZATION

Micro penetration knowledge in the whole field is very broad. In order to deal with the conditions of different sample research methods, people in the medium of the pore, in order to simulate the system scheme and develop a variety of physical samples, get the detailed and accurate research results of the actual situation underground, please approach as close as possible. According to the requirements of the research content, based on the completion of specific light transmittance, people show the pores from various angles, in order to simulate the microscopic implementation of the system penetration method, in order to explore the different fields of subtle penetration, various types of physical samples are developed. These physical samples can be roughly divided into the following four hours.

1) BEADED MODEL

Beaded samples have the characteristics of excellent light transmittance, relatively simple manufacturing process and reusability. Two glass plates are used to seal the carefully selected glass bead layer with the same material, leaving dike and ink, and to make layered porous media samples. Secondly, add samples in the center of two polished ceramic plates to make the glass and ceramic closer. If the above appropriate weight (metal block, etc.) is added, its weight is calculated according to the glass load of about 18G per 1 square centimeter. The effect of weight is evenly distributed on the whole sample and arranged on the resistance furnace. A central part more evenly distributed than the temperature. The purpose is to soften the hard glass and make the stool more firmly sintered. The electric furnace slowly heats up to the glass softening point in 1.5 hours and cuts off the power supply for natural cooling. After taking out, confirm the sintering state. Once the sintering fails, it can be burned again. Please refer to figure 4 below.

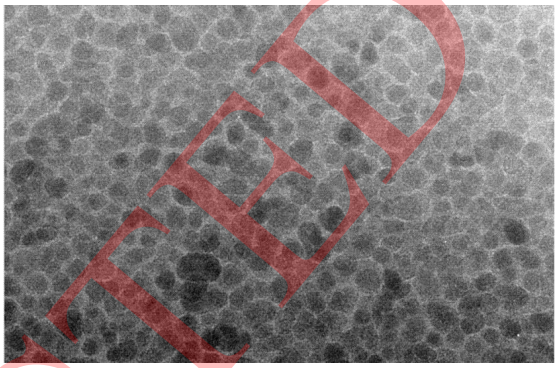

FIGURE 4. Diagram of non-melting particles under the bead model.

Figure 4 is a picture of the non molten particles under the bead sample. This kind of sintered glass has high light transmittance and can obtain clear and complete photos. It is suitable for the measurement of various interface phenomena, the study of various multiphase permeability and physical and chemical effects. After the post-processing, according to the specifications to form a variety of wettability, regeneration, upgrading and reuse, is a high applicability of the standard.

2) CAPILLARY NETWORK MODEL

This model investigates the movement of oil and water, most of which is carried out by pistons. At the same time, in the hydrophilic sample, the water can follow the water flow of the capillary wall. Using this sample and support requirements, we carried out an experimental study on the oil replacement mechanism of water attack method, bubble attack method, water reducing attack method and micro oil attack method, and achieved a series of results. The capillary network model is a two-dimensional through sample, which has the advantage of correctly setting the pore size and shape distribution of the pore system.

3) FINE PORE NETWORK MODEL

The fine pore network sample is a two-dimensional ruler sample which can simulate the three-dimensional dimension on a certain basis. It can meet the requirements of the medium's fine pore structure, especially the change characteristics of the fine pore throat. This two-dimensional transparent model is very suitable for auxiliary observation, so as to measure the position and movement of fluid in the channel. However, in this sample, it is still difficult to simulate the actual core and mineral composition, as well as the complex properties of the channel interior.

4) FINE PORE MODEL OF SANDSTONE

Sandstone fine pore sample is the micro sample of the actual reservoir fine pore structure. This is to wash the sliced mushroom, and then clip the cake between the two digit optical glass. The meter is sealed and the connection between the West and the outside is surrealistic. The advantage is that, because it is made of the actual core, it basically maintains the pore structure, morphology and mineral composition of the actual core. Pay attention to the production process, almost all the cement can be maintained. This can't be used on other models. The disadvantage of sandstone pore model is that the sample volume is small and the transmittance is low.

V. CONCLUSIONS

The development of image processing depends on the application and development of computer, among which the physical properties of carbon dioxide and mixtures below three key points are very incomplete. Therefore, this paper explores the visual experimental system, through the specific experimental operation and method optimization to study the process and phenomenon of carbon dioxide low-temperature condensation. Gas permeability has sliding effect, which is mainly reflected in different gas medium, different gas pressure and different permeability measured under different physical core conditions.

Based on MRI visualization technology, the permeability experiment of carbon dioxide immiscible phase drive in medium was carried out, and the mixed permeability of carbon dioxide in sand filled medium was observed. In the process of evolution, the effects of pressure, jet rate and pore structure of CO_2 immiscible flood are studied, which provides basic theoretical basis and technical support for the application of CO_2 EOR technology in industry in China.

For China's low transparency and low flow layer is the current development characteristics and recognition. Comprehensive analysis of the characteristics of various gases, introduction of gas through technology, and high efficiency of low permeability oil field, can not only achieve China's low permeability can improve the recovery rate of oil field, more conducive to sustainable development, but also help fundamentally solve the problem of China's ultra-low permeability oil field.

ACKNOWLEDGMENT

The authors would like to thank all editors and anonymous reviewers for their comments and suggestions.

REFERENCES

[1] X. Zhao, Y. Yao, and H. Ye, "The CO_2 storage and EOR evaluation in Daqing oilfield," *Greenhouse Gases: Sci. Technol.*, vol. 6, no. 2, pp. 251–259, 2016.
[2] E. M. Mirkes, A. N. Gorban, J. Levesley, P. A. S. Elkington, and J. A. Whetton, "Pseudo-outcrop visualization of borehole images and core scans," *Math. Geosci.*, vol. 49, no. 8, pp. 947–964, Nov. 2017.
[3] H. Zhao, Y. Chang, and S. Feng, "Oil recovery and CO_2 storage in CO_2 flooding," *Petroleum Sci. Technol.*, vol. 34, no. 13, pp. 1151–1156, 2016.
[4] Y. Li, J. Li, and S. Ding, "Co-optimization of CO_2 sequestration and enhanced oil recovery in extra-low permeability reservoir in Shanbei," *Energy Sources, A, Recovery, Utilization, Environ. Effects*, vol. 38, no. 3, pp. 442–449, 2016.
[5] Q. Cheng, Z. Li, G. Zhu, and H. Zhang, "Research and application of CO_2 flooding enhanced oil recovery in low permeability oilfield," *Open J. Geol.*, vol. 07, no. 09, pp. 1435–1440, 2017.
[6] P. Bakhshi, R. Kharrat, A. Hashemi, and M. Zallaghi, "Experimental evaluation of carbonated waterflooding: A practical process for enhanced oil recovery and geological CO_2 storage," *Greenhouse Gases: Sci. Technol.*, vol. 8, no. 2, pp. 238–256, 2018.
[7] M. Cui, R. Wang, and C. Lü, "Research on microcosmic oil displacement mechanism of CO_2 flooding in extra-high water cut reservoirs," *J. China Univ. Petroleum*, vol. 154, no. 1, pp. 119–125, 2017.
[8] D. Franz, F. Koebsch, and E. Larmanou, "High net CO_2 and CH_4 release at a eutrophic shallow lake on a formerly drained fen," *Biogeosciences*, vol. 13, no. 10, pp. 3051–3070, 2016.
[9] K. Yukiya and T. Toshifumi, "Synthesis of CO_2/N_2-triggered reversible stability-controllable Poly(2-(diethylamino)ethyl methacrylate)-grafted-AuNPs by surface-initiated atom transfer radical polymerization," *Langmuir*, vol. 30, no. 42, pp. 12684–12689, 2017.
[10] Z. Su, Y. Tang, and H. Ruan, "Experimental and modeling study of CO_2-Improved gas recovery in gas condensate reservoir," *Petroleum*, vol. 3, no. 1, pp. 87–95, 2016.
[11] A. K. M. Oliveira and S. C. J. Gualtieri, "Gas exchange in young plants of Tabebuia aurea (Bignoniaceae Juss.) subjected to flooding stress," *Revista Árvore*, vol. , 40, no. 1, pp. 39–49, 2016.
[12] F. Jin, Z. Liu, W. Pu, D. Zhong, C. Yuan, and B. Wei, "Experimental study of *in-situ* CO_2 foam technique and application in yangsanmu oilfield," *J. Surfactants Detergents*, vol. 19, no. 6, pp. 1231–1240, Nov. 2016.
[13] Y. Sun, Z. Du, L. Sun, and Y. Pan, "Phase behavior of $SCCO_2$ sequestration and enhanced natural gas recovery," *J. Petroleum Explor. Prod. Technol.*, vol. 7, no. 4, pp. 1085–1093, Dec. 2017.
[14] C. Deshmukh, F. Guérin, and A. Vongkhamsao, "Carbon dioxide emissions from the flat bottom and shallow Nam Theun 2 Reservoir: Drawdown area as a neglected pathway to the atmosphere," *Biogeosciences*, vol. 15, no. 6, pp. 1775–1794, 2017.
[15] L. Jun, Z. Junhua, and T. Mingyou, "Research status of CO_2 flooding and its seismic monitoring technologies," *Lithologic Re-Servoirs*, vol. 28, no. 1, pp. 128–134, 2016.
[16] N. Okorie, "The role of trees and plantation agriculture in mitigating global climate chang," *Afr. J. Food, Agricult., Nutrition Develop.*, vol. 17, no. 4, pp. 12691–12707. 2017.
[17] A. R. C. Morais, J. Andreaus, and R. Bogel-Lukasik, "Green and efficient approach to selective conversion of xylose and biomass hemicellulose into furfural in aqueous media using high-pressure CO_2 as a sustainable catalyst," *Green Chem.*, vol. 18, no. 10, pp. 2985–2994, 2016.
[18] Q. Luo and W. Song, "Preliminary research on visualization of S&T policy—A case study of China innovation and entrepreneurship graphic policies," *Open J. Social Sci.*, vol. 4, no. 5, pp. 135–143, 2016.
[19] L.-K. Shi, H. Zhou, and W.-H. Liu, "Multi-feature fusion and visualization of pavement distress images based on manifold learning," *J. Highway Transp. Res. Develop.*, vol. 11, no. 1, pp. 14–22, Mar. 2017.
[20] N. Jaccard, N. Szita, and L. D. Griffin, "Trainable segmentation of phase contrast microscopy images based on local basic image features histograms," *Comput. Methods Biomech. Biomed. Eng. Imag. Vis.*, vol. 5, no. 5, pp. 359–367, 2017.
[21] S. Jeon, "A method for the visualization of the deliberative process in urban environment improvement project: Focused on the Dongseong-ro public design improvement project in Dae-Gu, South Korea," *J. Archit. Planning*, vol. 82, no. 738, pp. 1999–2009, 2017.
[22] M. Liu, J. Shi, Z. Li, C. Li, J. Zhu, and S. Liu, "Towards better analysis of deep convolutional neural networks," *IEEE Trans. Vis. Comput. Graphics*, vol. 23, no. 1, pp. 91–100, Jan. 2017.
[23] G. Nidhi, "Despeckling of medical ultrasound images: A technical review," *Int. J. Inf. Eng. Electron. Bus.*, vol. 8, no. 3, pp. 11–19, 2017.
[24] T. Miao, X. Guo, W. Wen, and C. Wang, "3D appearance modeling and visualization of maize leaf with agronomic parameters," *Trans. Chin. Soc. Agricult. Eng.*, vol. 33, no. 19, pp. 187–195, 2017.
[25] X. Guo, Z. Yu, S. B. Kang, H. Lin, and J. Yu, "Enhancing light fields through ray-space stitching," *IEEE Trans. Vis. Comput. Graphics*, vol. 22, no. 7, pp. 1852–1861, Jul. 2016.

JIE CHI received the bachelor's degree in computational mathematics from the China University of Petroleum (East China), the master's degree in fundamental mathematics from the Chengdu University of Information Technology, and the Ph.D. degree in petroleum and natural gas engineering from the School of Energy Resources, China University of Geosciences, Beijing. He is currently an Associate Professor with the School of Basic Sciences, Shengli College, China University of Petroleum. His primary research interests include variable reservoir property seepage mechanics theory and application, numerical simulation, and CO_2 EOR.

JIABEI WANG received the bachelor's degree in exploration technology and engineering from Yangtze University, the master's degree in seismic exploration from the China University of Petroleum, Beijing, and the Ph.D. degree in mineral survey and exploration from the School of Energy Resources, China University of Geosciences, Beijing. She is currently a Lecturer with the Department of Earth Sciences, School of Petroleum and Natural Gas Engineering, Chongqing University of Science and Technology. Her primary research interests include reservoir prediction, fracture prediction, and seismic inversion.

XING ZHANG received the bachelor's degree in reservoir engineering from the School of Petroleum and Natural Gas Engineering, Chongqing University of Science and Technology and the master's and Ph.D. degrees in reservoir engineering from the Petroleum Department, China University of Petroleum (East China). He is currently a Professorate Senior Engineer with the Research Institute of Petroleum Engineering Technology, Shengli Oilfield Company, SINOPEC. His major research interests include oil reservoir protection, enhanced oil and gas recovery technology, and reservoir simulation.